
Article:
Dumitru, RB, Bissell, LA, Erhayiem, B et al. (11 more authors) (2021) Predictors of subclinical systemic sclerosis primary heart involvement characterised by microvasculopathy and myocardial fibrosis. Rheumatology, 60 (6). pp. 2934-2945. ISSN 1462-0324

https://doi.org/10.1093/rheumatology/keaa742

Supplementary file

Methods

CMR protocol

CMR studies were performed on a 3.0 T (Philips Achieva) equipped with a 32-channel receiver coil. Patients were asked to avoid caffeine for 24 hours prior to having the CMR performed.

Cine images

Scout images were used to plan cine images in the vertical long axis, pseudo short axis and horizontal long axis (balanced steady state free precession [bSSFP] acquisition). Cine image stack were acquired covering the entire heart. Image acquisition parameters for bSSFP as follows: TR 2.6 ms, TE 1.3 ms, flip angle 40°, spatial resolution 2.0 × 1.63 × 8 mm^3, 30 cardiac phases (1, 2).

T1 maps acquisition

Native and post contrast T1 mapping were planned in a single short axis slice at mid LV level using an ECG-triggered modified Look-Locker inversion (MOLLI) using the '3 of 5' approach, with 3x R-R interval recovery epochs, voxel size 1.7 x 2.14 x 10 mm^3 Trigger delay at end-diastole, flip angle 35°, FOV 320 – 420 mm (3, 4); Post-contrast T1 mapping was acquired 15 minutes after contrast administration.

First pass myocardial perfusion

Stress first-pass myocardial perfusion was acquired after intravenous adenosine administration (140 mcg/kg/min for three minutes) under continuous ECG monitoring and assessment for adequate haemodynamic response using a Gadolinium-DTPA (diethylene triamine pentaacetic acid (0.075 mmol/kg) bolus) for both stress and rest first-pass myocardial perfusion. A spoiled turbo gradient echo with a 5 × k-t Broad-use Linear Acquisition Speed-up Technique(BLAST), 11 training profiles, 1.31 × 1.32 × 10 mm^3 acquired resolution, pre-pulse delay of 100 ms, acquisition shot of 123 ms/slice, flip angle 20°, TR/TE 3.0/1.42 ms and three short axis slices was used (5).

Late gadolinium enhancement

Late gadolinium enhancement (LGE) images were acquired between 10 and 15 minutes following contrast administration using inversion recovery-prepared T1-weighted gradient echo. The optimal inversion time to null signal from normal myocardium was determined using a Look-Locker approach. 10 to 12 short axis slices were acquired, with further slices in the vertical and horizontal long axis orientations, or phase-swapped if indicated. Typical parameters for LGE images were as follows: TE 2.0 ms, TR 3.5 ms, flip angle 25°, acquired spatial resolution 1.54 × 1.76 × 10 mm.^{3}. Alternate heart beat acquisitions by navigator was used for poor breath holders.

CMR analysis

Image analysis was performed using cvi42 (v 5.6.5, Circle Cardiovascular Imaging Inc., Calgary, Canada) in accordance to recognised reporting standards(6) and using established and validated protocols.(7) LGE and myocardial perfusion were assessed by 2 blinded expert readers.

For LV volume and function, LV contours were drawn manually at both end diastole and end systole on the LV short axis SSFP cine stack.(6) Papillary muscles were included in the LV blood pool.

Native and post-contrast myocardial T1 was measured by delineating a region of interest in the mid interventricular septum(8) and in the LV blood pool. Care was taken to avoid partial-volume effects from neighbouring tissue or blood pool when delineating the region of interest (ROI). The following formula was used to calculate extracellular volume (ECV), where R1 is 1/T1, *myo pre* and *myo post* are the pre and post-contrast myocardial T1 values and *blood pre* and *blood post* are the pre-contrast and post-contrast blood pool T1 values.(9)

$$ECV = (1 - hematocrit) \times \frac{R1\ myo\ post - R1\ myo\ pre}{R1\ blood\ post - R1\ blood\ pre}$$

LGE was reported according to the 16 segment American Heart Association (AHA) model (10). The five-standard deviation (5SD) method was used for LGE scar mass quantification (11). Two separated

ROIs, one representing the region with LGE and the other representing remote myocardium, were delineated on the LGE short axis images to obtain the scar mass.

Perfusion was firstly assessed visually by comparing the rest and stress perfusion images using the 16 segment AHA model.(10)

Quantitative analysis of the perfusion data was performed to generate estimates of myocardial blood flow (MBF) at stress and rest as previously described. (12) Myocardial perfusion reserve (MPR) values were calculated by dividing the stress by the rest MBF. Breathing motion in the dynamic series was corrected using an automated registration algorithm (Circle Cardiovascular Imaging, Calgary, AB, Canada). Regions of interest defining the myocardium and a region within the left ventricular blood pool were then used to generate signal versus time curves. Signal values were converted to contrast agent concentrations using the pre-contrast T_1 measurements and the equation for the imaging sequence derived from the Bloch equations.(13, 14) The calibration factor S_0 was derived from the pre-contrast image signal (SI_{pre}) and pre-contrast T_1 (T_{1_pre}) as follows:

$$S_0 = \frac{SI_{pre}}{f(T_{1\_pre})}$$

Where *f(…)* denotes the equation describing the imaging pulse sequence.(13) The T_1 at each time point $T_1(t)$ was then obtained from the signal intensity *SI(t)*:

$$T_1(t) = min\left\{\left(S_0 . f\left(T_1(t)\right) - SI(t)\ \right)^2\right\}$$

The contrast agent concentration, *C(t),* was then obtained as follows:

$$C(t) = \frac{\frac{1}{T_{1(t)}} - \frac{1}{T_{1\_pre}}}{r_1}$$

Where r_1 is the contrast agent relaxivity.

The concentration versus time curves for the blood pool and myocardium were then used to estimate myocardial blood flow using model independent deconvolution.(14, 15) The following equation was minimized to find the flow weighted response function $R_f(t)$:

$$min\left\{\left\|A.R_f(t) - C_m(t)\right\|^2 - \lambda^2\left\|L.R_f(t)\right\|^2\right\}$$

A is the convolution matrix operator calculated form the arterial concentration curve(16) (4), C_m is the myocardial concentration versus time curve, L is the identity matrix and λ, is a coefficient that determines the degree to which the solution is forced to be smooth by the side constraint $\left\|LR_f\right\|^2$. The optimal value for λ was determined using the L-curve method. (14, 17) The MBF was taken as the maximum value of the flow weighted response function $Rf(t)$.

Results

One hundred and twenty-three SSc patients were screened for the study, out of whom twenty-nine were excluded as they did not meet the inclusion criteria or refused the CMR. Ninety-three patients were recruited but only eighty-three had CMR data available. Reasons for absent data is illustrated in figure 1. Of the eighty-three patients with CMR data, function/volume assessment was available for all patients, LGE-CMR and T1 native data was available for 80 patients, ECV% for 78 patients, perfusion data was available for 61 patients.

Figure S1. Flowchart showing patient selection, recruitment and feasibility

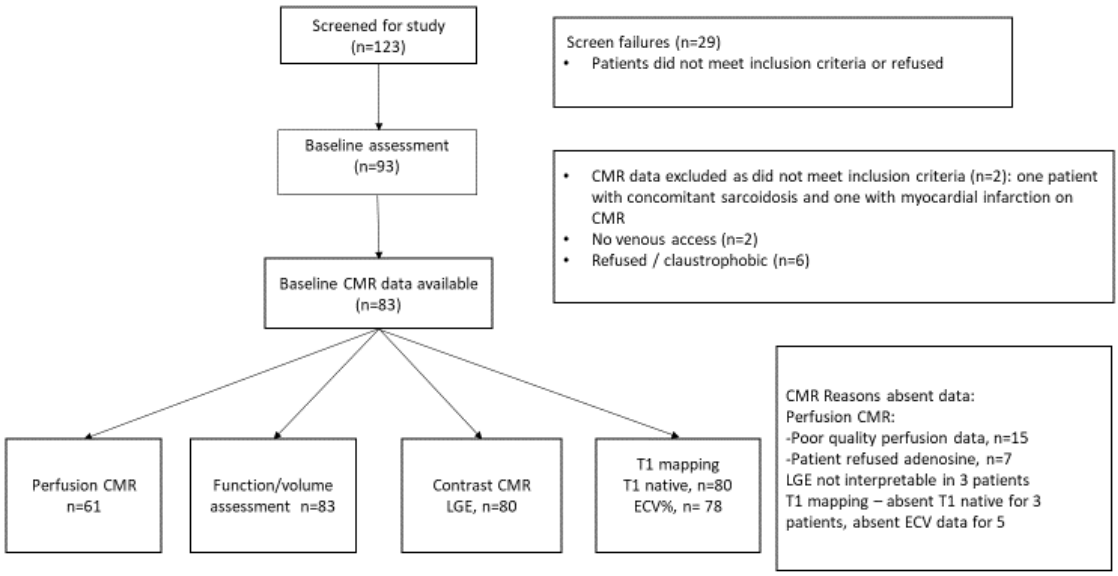
Screened for study
(n=123)
Screen failures (n=29)
• Patients did not meet inclusion criteria or refused
Baseline assessment
(n=93)
• CMR data excluded as did not meet inclusion criteria (n=2): one patient with concomitant sarcoidosis and one with myocardial infarction on CMR
• No venous access (n=2)
• Refused / claustrophobic (n=6)
Baseline CMR data available
(n=83)
CMR Reasons absent data:
Perfusion CMR:
-Poor quality perfusion data, n=15
-Patient refused adenosine, n=7
LGE not interpretable in 3 patients
T1 mapping – absent T1 native for 3 patients, absent ECV data for 5
Perfusion CMR
n=61
Function/volume
assessment n=83
Contrast CMR
LGE, n=80
T1 mapping
T1 native, n=80
ECV%, n= 78

Table S1. Standard of care cardio-pulmonary profile

Standard of care cardio-pulmonary profile (% predicted value)	
Forced vital capacity %, mean (SD)	101 (21)
Total lung capacity %, mean (SD)	92 (15)
DLCO %, mean (SD)	62 (14)
DLCO/VA %, mean (SD)	80 (15)
Cardiovascular risk profile, n%	
Dyslipidaemia	3 (4)
Hypertension	8 (10)
Smoking	7 (8)
Family history of CVD	8 (10)
Patients with any CV risk factors, n% 1 cv risk factor 2 cv risk factors	22 (27) 17 (21%) 5 (6%)
Systolic BP, mean (SD)	116 (16)
Diastolic BP, mean (SD)	67 (12)
BMI, median (IQR)	26 (20,31)
Cardiac serum biomarkers NT-proBNP, median (IQR) Hs-TnI, median (IQR) CK, median (IQR)	 92 (48,143) 4 (3,8) 73 (63,105)

BP, blood pressure; BMI, body mass index; CK, creatine kinase; CV, cardiovascular; CVD, cardiovascular disease; DLCO, diffusing capacity of the lungs for carbon monoxide; DLCO/VA, DLCO adjusted for volume; FVC, forced vital capacity; Hs-TnI, high-sensitivity troponin I; NT-proBNP, N-terminal pro brain natriuretic peptide; TLC, total lung capacity

Right ventricular (RV) dimension and function in SSc patients

RV parameters of SSc patients were within normal range, with a mean (SD) RVEF of 58 (7)%, RVED/ body surface area (BSA) of 79 (18), RVESV/BSA of 35 (12) and RVSV/ BSA of 46 (8) (ml/m^2).

Association between native T1 and clinical SSc phenotype

T1 native in SSc patients versus HC did not reach statistical significance, after applying Bonferroni correction. The association between T1 native and clinical phenotype is detailed in Table S2. T1 native associated with MRSS and had a negative association with dcSSc.

Table S2. Logistic and linear regression to predict the relationship between SSc clinical phenotype and native T1

Variable	**T1 native**			
	Linear univariate analysis		Multivariate analysis, R^2 =0.238	
	Beta	p value	Beta	p value
Male gender	-0.89	0.431	-0.194	0.129
Age	0.122	0.281		
Presence of CV risk factors	-0.081	0.475	-0.146	0.181
Disease duration	-0.076	0.508		
Presence of ILD	-0.151	0.181		
DLCO/VA	-0.054	0.641		
MRSS	0.249	0.026*	0.457	0.001*
DcSSc	-0.132	0.241	-0.312	0.015*
Digital ulcers	0.204	0.070	0.149	0.177
CRP	0.107	0.346	0.163	0.170
DMARD treatment	0.063	0.577		
ACE inhibitor treatment	-0.209	0.063		

* $p<0.05$; ** $p<0.001$

ACE, angiotensin converting enzyme; CV, cardiovascular; CRP, C-reactive protein; dcSSc, diffuse cutaneous systemic sclerosis; DLCO/VA, DLCO adjusted for volume; DMARD, disease modifying antirheumatic drugs; ECV, extracellular volume; ILD, interstitial lung disease; LGE, late gadolinium enhancement; MPR, myocardial perfusion reserve; MRSS, modified Rodnan skin score; OR odds ratio

Figure S2A. ROC curve of hs-TnI for predicting LGE. S2B ROC curve of NT-proBNP for predicting ECV (ECV <29; ECV≥29)

S2A

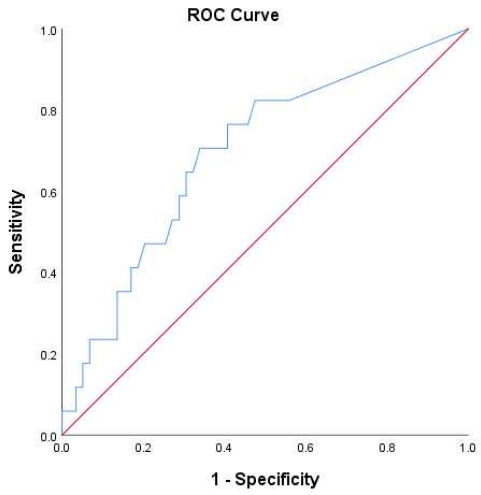

AUC (95%CI): 0.695(0.55, 0.837); p=0.015

S2B

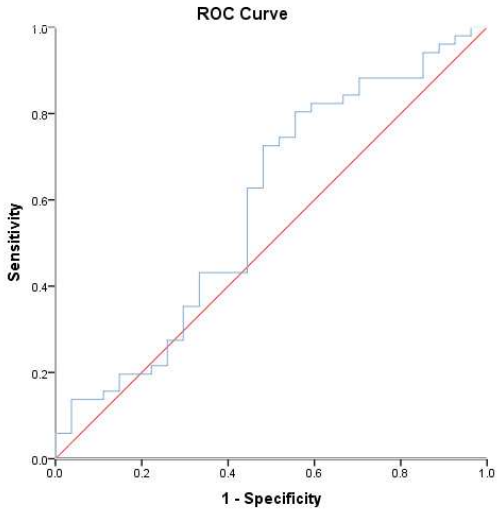

AUC (95%CI) =0.586 (0.447; 0.726);p=0.213

References

1. Alfakih K, Plein S, Thiele H, Jones T, Ridgway JP, Sivananthan MU. Normal human left and right ventricular dimensions for MRI as assessed by turbo gradient echo and steady-state free precession imaging sequences. Journal of Magnetic Resonance Imaging. 2003;17(3):323-9.

2. Burns J, Sivananthan MU, Ball SG, Mackintosh AF, Mary DASG, Greenwood JP. Relationship between central sympathetic drive and magnetic resonance Imaging-determined left ventricular mass in essential hypertension - Response. Circulation. 2007;116(17):E417-E.

3. Messroghli DR, Greiser A, Frohlich M, Dietz R, Schulz-Menger J. Optimization and validation of a fully-integrated pulse sequence for modified look-locker inversion-recovery (MOLLI) T1 mapping of the heart. Journal of Magnetic Resonance Imaging. 2007;26(4):1081-6.

4. Messroghli DR, Radjenovic A, Kozerke S, Higgins DM, Sivananthan MU, Ridgway JP. Modified Look-Locker inversion recovery (MOLLI) for high-resolution T-1 mapping of the heart. Magnet Reson Med. 2004;52(1):141-6.

5. Plein S, Ryf S, Schwitter J, Radjenovic A, Boesiger P, Kozerke S. Dynamic contrast-enhanced myocardial perfusion MRI accelerated with k-t sense. Magn Reson Med. 2007;58(4):777-85.

6. Schulz-Menger J, Bluemke DA, Bremerich J, Flamm SD, Fogel MA, Friedrich MG, et al. Standardized image interpretation and post processing in cardiovascular magnetic resonance: Society for Cardiovascular Magnetic Resonance (SCMR) Board of Trustees Task Force on Standardized Post Processing. Journal of Cardiovascular Magnetic Resonance. 2013;15(1):35.

7. Plein S, Ridgway JP, Jones TR, Bloomer TN, Sivananthan MU. Coronary artery disease: assessment with a comprehensive MR imaging protocol--initial results. Radiology. 2002;225(1):300-7.

8. Rogers T, Dabir D, Mahmoud I, Voigt T, Schaeffter T, Nagel E, et al. Standardization of T1 measurements with MOLLI in differentiation between health and disease - the ConSept study. Journal of Cardiovascular Magnetic Resonance. 2013;15(1):78.

9. Miller CA, Naish JH, Bishop P, Coutts G, Clark D, Zhao S, et al. Comprehensive validation of cardiovascular magnetic resonance techniques for the assessment of myocardial extracellular volume. Circulation Cardiovascular imaging. 2013;6(3):373-83.

10. Cerqueira MD, Weissman NJ, Dilsizian V, Jacobs AK, Kaul S, Laskey WK, et al. Standardized myocardial segmentation and nomenclature for tomographic imaging of the heart. A statement for healthcare professionals from the Cardiac Imaging Committee of the Council on Clinical Cardiology of the American Heart Association. Circulation. 2002;105(4):539-42.

11. McAlindon E, Pufulete M, Lawton C, Angelini GD, Bucciarelli-Ducci C. Quantification of infarct size and myocardium at risk: evaluation of different techniques and its implications. European heart journal cardiovascular Imaging. 2015;16(7):738-46.

12. Bissell LA, Dumitru RB, Erhayiem B, Abignano G, Fent G, Kidambi A, et al. Incidental significant arrhythmia in scleroderma associates with cardiac magnetic resonance measure of fibrosis and hs-TnI and NT-proBNP. Rheumatology (Oxford). 2019.

13. Broadbent DA, Biglands JD, Ripley DP, Higgins DM, Greenwood JP, Plein S, et al. Sensitivity of quantitative myocardial dynamic contrast-enhanced MRI to saturation pulse efficiency, noise and t1 measurement error: Comparison of nonlinearity correction methods. Magn Reson Med. 2016;75(3):1290-300.

14. Biglands JD, Magee DR, Sourbron SP, Plein S, Greenwood JP, Radjenovic A. Comparison of the Diagnostic Performance of Four Quantitative Myocardial Perfusion Estimation Methods Used in Cardiac MR Imaging: CE-MARC Substudy. Radiology. 2015;275(2):393-402.

15. Pack NA, DiBella EV. Comparison of myocardial perfusion estimates from dynamic contrast-enhanced magnetic resonance imaging with four quantitative analysis methods. Magnetic resonance in medicine. 2010;64(1):125-37.

16. Jerosch-Herold M, Swingen C, Seethamraju RT. Myocardial blood flow quantification with MRI by model-independent deconvolution. Medical physics. 2002;29(5):886-97.

17. Christian HP. Rank-Deficient and Discrete ill-posed Problems. Numerical Aspects of Linear Inversion. SIAM monographs on Mathematical Modeling and Computation (Society for Industrial and Applied Mathematics); 1998.